Reynolds number dependence of heavy particles clustering in homogeneous isotropic turbulence

Xiangjun Wang,[1,2] Minping Wan,[2,*] Yan Yang,[2] Lian-Ping Wang,[2,3] and Shiyi Chen[2]

[1]*Harbin Institute of Technology, Harbin, Heilongjiang, 150090, China*

[2]*Guangdong Provincial Key Laboratory of Turbulence Research and Applications, Department of Mechanics and Aerospace Engineering, Southern University of Science and Technology, Shenzhen, Guangdong, 518055, China*

[3]*Department of Mechanical Engineering, 126 Spencer Laboratory, University of Delaware, Newark, Delaware 19716-3140, USA*

(Received 2 June 2020; accepted 24 September 2020; published 14 December 2020)

The preferential concentration of heavy inertial point particles in homogeneous isotropic turbulence is investigated with direct numerical simulations. The particle clustering is measured by the standard deviation of normalized Voronoï volumes. With the particle number, large-scale time and length fixed, it is found that the degree of particle clustering is reduced with the increase of Taylor Reynolds number (R_λ) for $52 \leqslant R_\lambda \leqslant 139$ when the Stokes number (St) is small (e.g., St <2.0), where St is the ratio of particle response time (τ_p) to the Kolmogorov timescale (τ_η). On the contrary, the clustering of high-St particles tends to become stronger with the increase of R_λ in the same R_λ range. Quantities invoked for low-St particle clustering include τ_η, the characteristic time (τ_f) of particles being trapped by "shear structures" and the strength of "shear structures" quantified by the second invariant of velocity gradient tensor ($Q = S_{ij}S_{ij} - \Omega_{ij}\Omega_{ij}$). While the increase of Q with Reynolds number enhances preferential concentration, τ_η and τ_f both decrease as Reynolds number increases, which could moderate the level of particle clustering. Then the observable reduction in the clustering of low-St particles with increasing R_λ emerges as the dominance of τ_η and τ_f over Q effects. In addition, we find that the strain rate cannot directly affect the spatial inhomogeneous distribution of low-St particles, but instead it impacts low-St particle clustering indirectly due to its correlation with the rotation rate. Unlike low-St particles dominated by small-scale eddies, the clustering of high-St particles is mainly influenced by large-scale eddies due to the "resonant" effect between particles and eddies.

DOI: 10.1103/PhysRevFluids.5.124603

I. INTRODUCTION

Multiphase flows are quite common in nature and engineering application, such as cloud-droplet growth, sandstorm transport, plankton distribution, spray combustion, and aerosol manufacturing. In the past decades, many investigations have been carried out to explore these complex phenomena. This paper focuses on the preferential concentration of heavy inertial particles of size much smaller than the Kolmogorov scale, suspended in three-dimensional (3D) incompressible homogeneous isotropic turbulence (HIT).

In the exploration of particle-laden turbulence, the establishment of the Maxey-Riley-Gatignol equation of motion for a small solid particle in a turbulent flow [1,2] was a milestone bringing

*wanmp@sustech.edu.cn

together previous investigations [3–10] for various forces acting on a particle, on a firm mathematical framework. A few years later, Maxey [11] pointed out that the velocity of small heavy particles ($\mathbf{v}_p$) could be approximately formulated as $\mathbf{v}_p = \boldsymbol{u}_p - \tau_p \boldsymbol{a}$ when the Stokes number is much smaller than unity, where $\boldsymbol{u}_p$ and $\boldsymbol{a}$ are the fluid velocity and acceleration at the position of particles, respectively, and τ_p is the particle response time. Then, the distribution of particles could be regarded as a continuous field. The divergence of $\mathbf{v}_p$, therefore, could be expressed as $\nabla \cdot \mathbf{v}_p = -\tau_p(S_{ij}S_{ij} - \Omega_{ij}\Omega_{ij})$, where S_{ij} and Ω_{ij} are the rate-of-strain tensor and rate-of-rotation tensor, respectively. Namely, heavy particles tend to collect in the region of high strain rate and low rotation rate. Squires and Eaton [12] verified the existence of preferential concentration of heavy particles in turbulence with direct numerical simulations.

Since then, interests surged and sustained as to the mechanisms leading to particle preferential concentration, for different particle Stokes numbers under different flow conditions. Maxey [11] attributed the particle clustering to the centrifugal effect owing to the difference of inertia between particles and fluids. Coleman and Vassilicos [13] demonstrated that the centrifugal mechanism dominates the preferential concentration of particles only in the limit of St $\ll 1$, but it is also accepted that centrifugal forces still have an impact on the clustering of particles until St approaching to 1 [13–15]. Furthermore, Bragg *et al.* [16,17] pointed out that a history effect of particle inertia would play a more important role when St $\geqslant O(1)$. Falkovich *et al.* [18] proposed that "sling effect" (also called fold caustic) mechanism should play an important role in facilitating the collision of particles. Bec *et al.* [19] also emphasized that "sling effect" could substantially increase the collision rates of particles. Subsequently, Wilkinson and Mehlig [20] and Wilkinson *et al.* [21] made a detailed analysis on the caustic mechanism in particle clustering. They found that caustic curves could precisely describe the regions of high concentration particles in a randomly moving fluid. Chun *et al.* [22] declared that there are two mechanisms contributing to the spatial inhomogeneous distribution of small heavy particles in the sub-Kolmogorov length scale. One is the radial inwards drift between particles arising from the particle inertia, which increases linearly with the inter-particle distance. The other is the pairwise diffusion of particles induced by the diffusivity of turbulence, which varies with the quadratic of particle distances. The radial distribution function (RDF) of particles follows a power law in the sub-Kolmogorov range, which is determined by these two factors. Here, the RDF is defined as $g(r) = (N_r V_t)/(N_t V_r)$, where N_r is the number of particle pairs separated by a distance r. V_r is the volume of a thin spherical shell with radius of r and thickness of dr. N_t and V_t are the total number of particle pairs and the total volume of computational domain, respectively. Another statistical model of particle clustering is introduced by Zaichik and Alipchenkov [23], wherein they successfully predicted the RDF of particles in isotropic turbulence based on the probability density function (PDF) of the relative velocity of two particles. The results in Refs. [22] and [23] are consistent with each other when St is much smaller than unity. A comparison of the two models made by Bragg and Collins [24] showed that the model proposed by Chun *et al.* [22] is a good approximation, to the leading order, of that by Zaichik and Alipchenkov [23], the latter thus being applicable to a wider range of St. Additionally, Goto and Vassilicos [25] proposed a "sweep-stick" mechanism that the position of heavy particles suspended in turbulence coincides with the location of acceleration stagnation points in two-dimensional (2D) homogeneous isotropic turbulence, whereas in 3D turbulence, it is in good agreement with those points with $\boldsymbol{e}_1 \cdot \boldsymbol{a} = 0$, where $\boldsymbol{a}$ is the fluid acceleration and $\boldsymbol{e}_1$ is the eigenvector of the symmetric part of the acceleration gradient tensor ($\nabla \boldsymbol{a}$), corresponding to the largest positive eigenvalue. Coleman and Vassilicos [13] developed a generalized "sweep-stick" mechanism applicable to the preferential concentration of heavy particles in 2D and 3D HIT, correcting the previous work by Goto and Vassilicos [25]. They pointed out that heavy particles also preferentially stick to the points with $\boldsymbol{a} = 0$ in 3D HIT, instead of those points with $\boldsymbol{e}_1 \cdot \boldsymbol{a} = 0$.

While the earlier works [26–28] revealed that the small-scale eddies are mainly responsible for the preferential concentration of inertial particles, later investigations [29–32] suggested that the preferential concentration of inertial particles is a multi-scale phenomenon when the flow Reynolds number is large. In particular, it is scale-dependent in the inertial range. Furthermore, Yoshimoto and Goto [29] pointed out that the distribution of particles in HIT is self-similar.

Besides the physical mechanisms of particle clustering, there have been various efforts to describe Reynolds number dependence of the preferential concentration. Wang *et al.* [28] studied the collision rate of small heavy particles suspended in turbulence with R_λ from 24 to 75. They concluded that the RDF of particles at contact is independent of R_λ when St is much smaller than unity. In contrast, it increases piecewise linearly with Reynolds number when $\mathrm{St} > 0.5$. The correlation dimension (D_2) of particles, a way to measure the level of the preferential concentration of particles, is found to be independent of the Reynolds number [30,33]. This might be due to the fact that D_2 only describes the distribution of particles in the dissipation range where effects of Reynolds number are negligible. However, the degree of preferential concentration of particles, in terms of pair correlation function, gradually increases with Reynolds number until it saturates at $R_\lambda \approx 100$ [34]. The higher St, the more sensitive particles clustering to Reynolds number. In addition, Rosa *et al.* [35] presented that the RDF of particles at contact reaches a peak near $R_\lambda = 100$ and then reduces slightly in some cases when R_λ is approximately larger than 200. However, Rosa *et al.* [35] fixed the diameter of particles instead of the Stokes number. The flow Reynolds number is not the only governing parameter, which explains some discrepancies in different studies. Onishi *et al.* [36] appealed to the the intermittency of turbulence to explain the Reynolds number dependence of particles clustering, and provided a systematical analysis by means of the local strain rate [15], an aspect which will be revisited in more detail in section 3.2. Sumbekova *et al.* [37] carried out a series of experiments to study the dependence of preferential concentration of sub-Kolmogorov particles on the Stokes number and flow Reynolds number when $\mathrm{St} = 0.5 \sim 5$ and $R_\lambda = 170 \sim 450$. They revealed that the standard deviation of the normalized areas of Voronoï polygons yields a power law dependence on Reynolds number with the exponent of 0.97.

In spite of the large amount of studies on particle clustering, one may observe from the aforementioned brief review that there is a lack of consensus on a couple of issues, for example, the Reynolds number dependence of the preferential concentration of heavy particles and the ambiguities surrounding the precise mechanisms of particle clustering.

In this paper, we mainly pay attention to the Reynolds number effects on the spatial inhomogeneous distribution of heavy inertial point particles in homogeneous isotropic turbulence with particle number fixed. We also propose a plausible explanation to the Reynolds number dependence of particle clustering. The outline of this paper is as follow: The simulation configuration is introduced in Sec. II. The mechanism for the Reynolds number dependence of the preferential concentration of particles is described in Sec. III. Finally, a brief conclusion and discussion is presented in Sec. IV.

II. SIMULATION CONFIGURATION

A series of numerical simulations on three-dimensional incompressible HIT laded with inertial particles have been conducted. The dynamics of fluid is governed by the mass equation and momentum equations,

$$\nabla \cdot \boldsymbol{u} = 0, \tag{1}$$

$$\frac{\partial \boldsymbol{u}}{\partial t} + \boldsymbol{u} \cdot \nabla \boldsymbol{u} = -\frac{1}{\rho}\nabla p + \frac{\mu}{\rho}\nabla^2 \boldsymbol{u} + \boldsymbol{f}, \tag{2}$$

where $\boldsymbol{u}$, ρ, p, and μ are, respectively, the velocity, fluid density, pressure, and dynamic viscosity. Here an external force $\boldsymbol{f}$ is imposed at large scales to achieve a stationary state, which is accomplished by keeping constant the kinetic energy at the first two wave number shells. We solve the above equations in Fourier space via a pseudospectral method [38,39] with second-order Adams-Bashforth time stepping [40,41] in a periodic cube of size 2π and with numerical resolution of 512^3 grid points. The aliasing error is removed by a combination of phase shift and truncation, so that the largest magnitude of the wave vectors resolved in our simulations $k_{\max} \sim 240$. The

TABLE I. Simulation parameters: Taylor Reynolds number R_λ, grid points N^3, kinematic viscosity ν, dissipation rate $\varepsilon = 2\nu\langle S_{ij}S_{ij}\rangle$, Kolmogorov length scale η, Kolmogorov timescale τ_η, root-mean-square fluctuation velocity $u_{\rm rms}$, integral length scale L_f, and large-scale eddy turnover time T_f.

R_λ	N^3	ν	ε	η	τ_η	$u_{\rm rms}$	L_f	T_f
52	512^3	0.0090	0.10	0.052	0.30	0.63	1.61	2.53
89	512^3	0.0035	0.12	0.024	0.17	0.69	1.41	2.03
104	512^3	0.0026	0.12	0.019	0.14	0.70	1.40	2.01
121	512^3	0.0020	0.12	0.016	0.13	0.69	1.39	2.02
139	512^3	0.0015	0.12	0.013	0.11	0.70	1.35	1.93

velocity field is initialized with random phases and fluctuation amplitudes. The above implies that both the root-mean-square fluctuation velocity $u_{\rm rms} = \sqrt{\langle u_i u_i\rangle/3}$, the integral length scale $L_f = \pi/(2u_{\rm rms}^2)\int[E(k)/k]dk$ and large-scale eddy turnover time $T_f = L_f/u_{\rm rms}$ of the flows are more or less fixed. Other relevant parameters of simulations are listed in Table I.

One million particles are uniformly released into the flow once the turbulence reaches a statistically stationary state and then evolve for at least 20 large eddy turnover times. The motion of inertial pointlike particles is governed by

$$\frac{d\boldsymbol{x}_p}{dt} = \mathbf{v}_p, \tag{3}$$

$$\frac{d\mathbf{v}_p}{dt} = \frac{\boldsymbol{u}_p - \mathbf{v}_p}{\tau_p}, \tag{4}$$

where $\boldsymbol{x}_p$ and $\mathbf{v}_p$ represent the position and velocity of particles, respectively. $\boldsymbol{u}_p$ denotes the fluid velocity at the position of particles, which is computed by a sixth-order Lagrangian interpolation. We avoid some complications here, such as the impact of particles on turbulence and collisions among particles, since the particle size is much smaller than the Kolmogorov length scale (η) of turbulence and particles only occupy a small portion of the whole domain. Moreover, only the Stokes drag is retained in the dynamic equations for particles. Other forces such as added mass force and Basset-history force are not considered. The particle response time reads $\tau_p = 2\rho_p a^2/[9\mu(1+0.15\mathrm{Re}_p^{0.689})]$ [42], with Re_p being the Reynolds number of particles, a the particle radius, and ρ_p the particle density, which is much higher than the fluid density, typically of the order one thousand times the fluid density. We use at least 20 time slices over 10 large eddy turnover times to obtain relevant statistics. To investigate the Reynolds number dependence of particle clustering, five series of runs with varying Taylor Reynolds number R_λ from 52 to 139 are conducted. Here, R_λ is an average value of Taylor Reynolds numbers at a sequence of time slices, with an error range less than $\pm 4.0\%$ for each case. Also, the particle Stokes numbers vary in the range of $0 \leqslant \mathrm{St} \leqslant 6.40$ in all simulations (error range of St less than $\pm 8.0\%$ for each case).

III. RESULTS AND ANALYSIS

In this section, we present the Voronoï analysis for particle clustering followed by detailed explanations of Reynolds number dependence of high- and low-St inertial particle clustering.

A. Reynolds number dependence by Voronoï analysis

There are various diagnostics, depending on the scales and properties concerned, that are relevant to the assessment of the degree of particle clustering. In this paper, we employ the Voronoï method [14,43–46] to measure the preferential concentration of inertial particles. The computational domain is divided into a number of Voronoï cells associated to each particle, and one Voronoï cell only

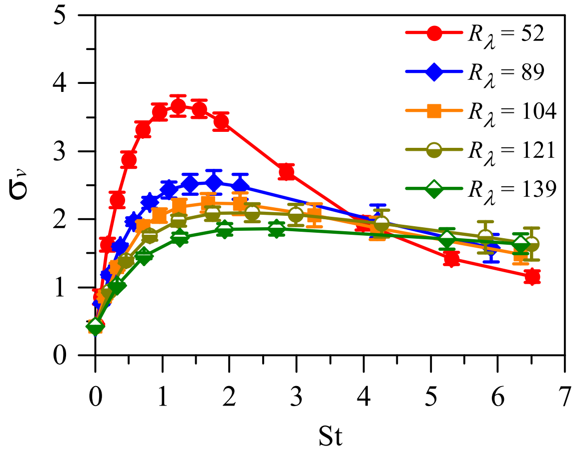

FIG. 1. The standard deviation σ_v for varying St at $R_\lambda = 52 \sim 139$.

contains the spacial points that are closer to its own particle than to any other. If particles are distributed close to each other, then the volumes of corresponding Voronoï cells (V) will be small, and vice versa. Therefore, the standard deviation of the volumes of Voronoï cells can quantify the degree of particle preferential concentration.

To remove possible influence of particle number (N_p) on statistics, we normalize the Voronoï volumes (V) by their averaged volume ($\langle V \rangle$), $\widetilde{\mathcal{V}} = V/\langle V \rangle$. As a first diagnostic to address the Reynolds number dependence of particle clustering, Fig. 1 shows the standard deviation of $\widetilde{\mathcal{V}}$, σ_v, for varying St at $R_\lambda = 52 \sim 139$. The first thing to notice is that the curves peak near St $= O(1)$ [26,47–49] and the Stokes number where σ_v peaks seems to increase with increasing R_λ. Also noteworthy is that for low St, approximately St <2.0 in present simulations, σ_v becomes remarkably attenuated as R_λ increases, while it is enhanced for high St. This can be verified in Fig. 2, where particle distributions in the same slice are shown for St ≈ 1.25 and St ≈ 6.40 at $R_\lambda = 52$, 104, and 139. Throughout the paper, all particles lying close to the 2D slice, e.g., less than the Kolmogorov length scale η in the perpendicular direction, are projected into the 2D slice to obtain particle distribution. In the low St cases, as shown in Figs. 2(a)–2(c), particles populate in narrow but long lanes at $R_\lambda = 52$, which, however, appear to be a collection of short and broken portions as R_λ increases, see for example Fig. 2(c). However, in the high St cases, e.g., St ≈ 6.40 presented in Figs. 2(d)–2(f), it can be visually found that the particle clustering is enhanced with increasing R_λ. Therefore, we close this section with a salient point of this paper: the preferential concentration of heavy inertial particles with low St attenuates with Reynolds number in the range of $R_\lambda = 52 \sim 139$, whereas that of high-St particles is enhanced with increasing Reynolds number.

Tagawa *et al.* [14] discovered σ_v also depends on the number of particles, even though the Voronoï volumes have been normalized. Whereafter, Monchaux [50] described that the dependence of σ_v on particle number was attributed to the different probing scales for different particle number. We investigate this uncertainty in Fig. 3(a), which exhibits that σ_v keeps increasing with the increase of particle number at $R_\lambda = 52$, 104, and 139. It is known that, as particle number changes, the probability density functions (PDFs) of $\widetilde{\mathcal{V}}$ for randomly distributed particles are in the same form, which yields a Gamma distribution [43]. σ_v is therefore independent of the particle number. However, this does not hold if particles accumulate preferentially. Figure 3(b) shows the PDFs of the normalized Voronoï volume, $\widetilde{\mathcal{V}}$, for different particle numbers at St ≈ 1.25 and $R_\lambda = 104$. One can see that the case with larger particle number has a higher probability for both small and large $\widetilde{\mathcal{V}}$, which leads to larger σ_v. Fortunately, σ_v changes with Reynolds numbers in a similar way for any fixed number of particles, as shown in Fig. 3(a). Throughout this paper all simulations are seeded with 10^6 particles to avoid being sidetracked by the possible effect of particle number.

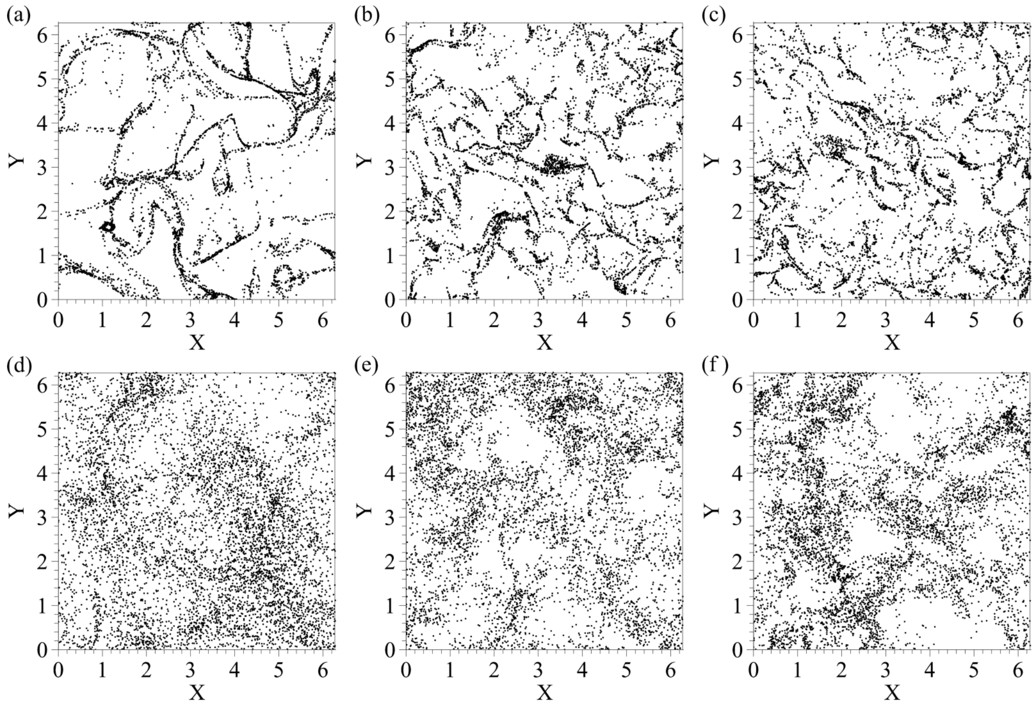

FIG. 2. Particle positions in the same 2D slice are shown for St ≈1.25 at (a) $R_\lambda = 52$, (b) 104, and (c) 139; and for St ≈6.40 at (d) $R_\lambda = 52$, (e) 104, and (f) 139.

B. Reynolds number dependence at low St

In this subsection, we investigate the preferential concentration of inertial particles at low St. To this end, it is widely accepted that heavy particles preferentially accumulate in high-strain and low-rotation regions [11,12,51–53]. Onishi and Vassilicos [15] adapted this idea to explain the change in the preferential concentration with the increase of Reynolds number. They demonstrated that the case with higher Reynolds number corresponds to smaller fraction of region with high normalized

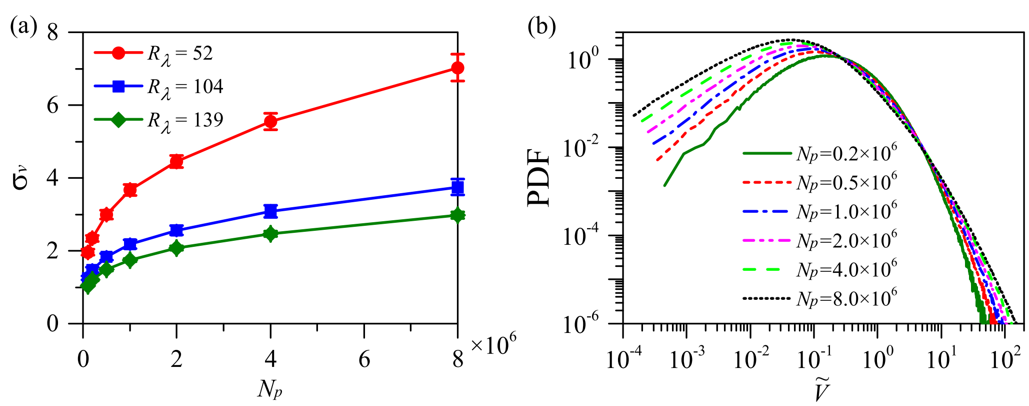

FIG. 3. (a) The standard deviation of nondimensional Voronoï volumes ($\widetilde{\mathcal{V}}$), σ_v, varies with particle number (N_p) when St ≈1.25 at $R_\lambda = 52$, 104, and 139. (b) The probability density functions (PDFs) of $\widetilde{\mathcal{V}}$ for different particle numbers at St ≈1.25 and $R_\lambda = 104$.

TABLE II. The cases at St $\approx$1.25 with $R_\lambda = 52 \sim 139$: space-time average values of the strain rate $\langle s^* \rangle$, the strain rate at the position of particles $\langle s_p^* \rangle$, the rotation rate $\langle r^* \rangle$, and the rotation rate at the position of particles $\langle r_p^* \rangle$.

R_λ	$\langle s^* \rangle$	$\langle s_p^* \rangle$	$\langle r^* \rangle$	$\langle r_p^* \rangle$
52	2.16	2.20	2.00	1.53
89	3.67	3.72	3.35	2.53
104	4.29	4.43	3.88	3.02
121	4.73	4.77	4.29	3.27
139	5.60	5.64	5.07	3.86

strain rate, $\sigma^* = s^*/\langle s^* \rangle$ (where $s^* = \sqrt{2S_{ij}S_{ij}}$ and $\langle \cdot \rangle$ denotes the ensemble average), and therefore the particle clustering is weakened.

Here we make a comparison between the strain rate s^* (the rotation rate $r^* = \sqrt{2\Omega_{ij}\Omega_{ij}}$) and its localized value at the position of particles s_p^* (its localized value r_p^*). Shown in Table II are the cases at St $\approx$1.25 for clarity, and the results of other cases in our paper are consistent with the listed ones. One can see that $\langle r_p^* \rangle$ is smaller than $\langle r^* \rangle$ by about 20%, which is in favor of the particle preferential concentration in relatively low-rotation regions. However, and perhaps most remarkably, there is no much larger $\langle s_p^* \rangle$ as compared to $\langle s^* \rangle$, as there should have been if particles tend to accumulate in high-strain regions. The PDFs of s^*, s_p^*, r^* and r_p^* in Fig. 4 add more evidence to the finding of Table II, wherein the PDFs of s^* and s_p^* almost collapse with each other, while the PDF of r_p^* shifts left in comparison with r^*. The particle distributions are plotted on the top of the color maps of the strain rate s^* and the rotation rate r^* in Fig. 5. No apparent associations between particle clustering and high strain rate can be observed in Fig. 5(a), while we can readily identify the preferential concentration of particles in regions of low rotation rate in Fig. 5(b).

The aforementioned results suggest that low-St particle clustering needs not be associated with high strain, but rather occurs preferentially in low-rotation patches, which may seem at first to be in conflict with the argument that particles tend to accumulate in high-strain regions [11,12,51–53]. It may not be so surprising that there is a strong correlation between low rotation and particle concentration, since, at a heuristic level, heavy particles are expected to be expelled from vortices due to inertia. We reinterpret the role of strain on particle clustering to be indirect. In some studies [12,51–53], the correlation between high strain and particle concentration is not guaranteed mathematically, but emerges due to its possible superposition with low rotation. However, in our

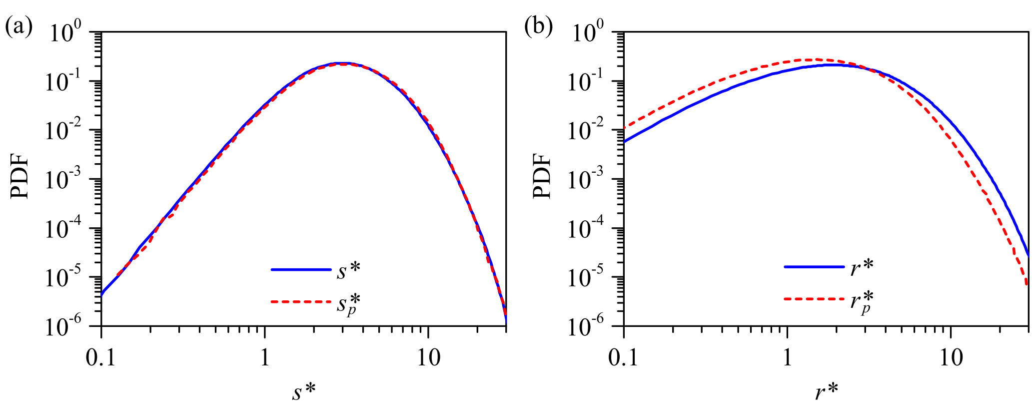

FIG. 4. PDFs of (a) the strain rate s^* and the strain rate at the position of particles s_p^*, and (b) the rotation rate r^* and the rotation rate at the position of particles r_p^* for St $\approx$1.25 at $R_\lambda = 104$.

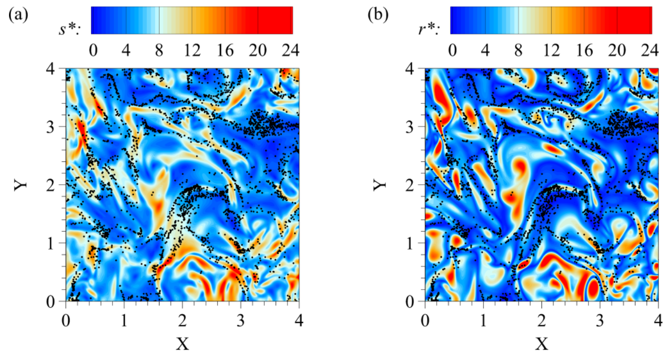

FIG. 5. Particle positions superposed on color maps of (a) the strain rate s^* and (b) the rotation rate r^* in a 2D subregion for St $\approx$1.25 at $R_\lambda = 104$.

HIT simulations, comparison of Figs. 5(a) and 5(b) reveals greatly similar patterns of large strain and large rotation. The high rotation rate is well associated with large strain rate [54]. However, they seem to be independent of each other in the region with low rotation rate (joint PDF not shown). As a consequence, particles will mainly populate in the region of low rotation rate, where the strain rate is independent of the rotation rate. This is intuitively consistent with the finding in Fig. 4(a), where the PDF of s^* then collapses onto that of s_p^*.

In addition to the preceding reasoning for the effect of coherent structures, we seek to appeal to the alternatives available for the Reynolds number dependence of low-St particle preferential concentration. Here we consider the particles as a continuous compressible flow and start with the particle number conservation equation,

$$\frac{\partial n}{\partial t} + \nabla \cdot (n\mathbf{v}_p) = 0, \tag{5}$$

where $n(\boldsymbol{x}, t)$ is the local particle number density. It can be expressed also in the form

$$\frac{\partial n}{\partial t} + \mathbf{v}_p \cdot \nabla n = -n\nabla \cdot \mathbf{v}_p. \tag{6}$$

A reasonable approximation for small Stokes number [11] is

$$\nabla \cdot \mathbf{v}_p = -\tau_p(S_{ij}S_{ij} - \Omega_{ij}\Omega_{ij}) = -\tau_p Q. \tag{7}$$

On plugging the above equation into Eq. (6), we have

$$\frac{dn}{dt} = n\tau_p Q, \tag{8}$$

where d/dt is defined as $\partial/\partial t + \mathbf{v}_p \cdot \nabla$. Integrating the above equation over time yields the time evolution of n, denoted by n_0 at initial time, which reads

$$n = n_0 e^{\tau_p \int_0^t Q d\tau}. \tag{9}$$

After the distribution of particles reaches a statistically stationary state, Q along particle trajectories, owing to the movement of vortices, will fluctuate around an average value with a characteristic period (τ_f) statistically, as shown in Fig. 6. Physically, τ_f can be regarded as the characteristic timescale over which particles are trapped by "shear structures." Here, "shear structures" refer the flow structures in the periphery of vortices. Therefore, the characteristic concentration of particles can be written as

$$n(\tau_f) = n_0 e^{\tau_\eta \tau_f \langle Q\rangle_l \mathrm{St}}, \tag{10}$$

where $\langle\cdot\rangle_l$ represents the average along Lagrangian particle trajectories.

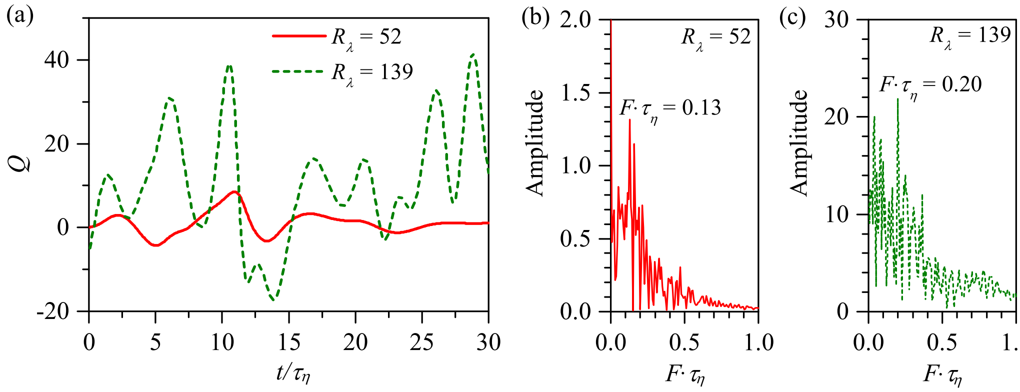

FIG. 6. Q along a typical particle trajectory at St ≈1.25: (a) short segments of time histories of Q at $R_\lambda = 52$ and 139, (b) frequency spectra of Q at $R_\lambda = 52$, (c) frequency spectra of Q at $R_\lambda = 139$.

According to Eq. (10), a point to be realized immediately is that, for any fixed St, $n(\tau_f)$ is related to $\langle Q\rangle_l$ as well as the Kolmogorov timescale τ_η, and the particle trapped time τ_f. In addition, when St is small enough, the contributions from τ_η, τ_f and $\langle Q\rangle_l$ are negligible, which implies that the preferential concentration of particles will become less sensitive to the Reynolds number. This can be seen in Fig. 1 where the data points start to collapse for quite small St. This point of view is also supported by Wang *et al.* [28], Zhou *et al.* [27], Onishi and Seifert [55]. It is known that τ_η decreases with the increase of R_λ when the integral scales are fixed, seen also in Table III, where relevant statistics at St $\approx$ 1.25 are shown. However, as R_λ increases, the value of Q in "shear structures" will also increase statistically, which results in the increase of $\langle Q\rangle_l$. Then the remainder that needs to be specified is τ_f. We present the time history and frequency spectra of Q along a typical particle trajectory at $R_\lambda = 52$ and 139 for reference in Fig. 6, wherein one can see immediately that the dominant fluctuating frequencies of Q at varying Reynolds numbers are quite different. We then apply the Fourier spectral analysis to the time series (more than eight large-scale eddy turnover times) of Q along hundreds of random selected particle trajectories, and the average characteristic frequency (F) is taken as the arithmetical mean of the frequency of each time series of Q at which the mode gets the largest amplitude. Seen in Table III is that the average particle trapped time $\tau_f = 1/F$ decreases with increasing R_λ. Moreover, from Table III, the variables: $\tau_\eta R_\lambda$ and $\langle Q\rangle_l/(R_\lambda)^2$ are roughly constant with the increase of R_λ, whereas $\tau_f R_\lambda$ decreases. Here, the first relation apparently results from the roughly fixed τ_f. For the last two relations, we only show that they hold for our numerical simulation, but a physical interpretation is yet to be discovered. In summary, our results signify a pathway by which the three parameters—τ_η, τ_f and $\langle Q\rangle_l$—act in concert and eventually lead to decreasing $\tau_\eta\tau_f\langle Q\rangle_l$ with increasing R_λ (see Table III), thus providing a plausible explanation

TABLE III. Characteristic quantities at St ≈1.25 with $R_\lambda = 52 \sim 139$. $\langle Q\rangle_l$ is the Lagrangian averaged Q along particle trajectories. F is the average characteristic frequency of the time series of Q along particle trajectories. τ_f represents the characteristic timescale of particles being trapped by "shear structures."

R_λ	τ_η	$\langle Q\rangle_l$	F	τ_f	$\tau_\eta\tau_f\langle Q\rangle_l$	$\tau_\eta^2\langle Q\rangle_l$
52	0.303	2.541	0.465	2.149	1.656	0.234
89	0.170	7.659	0.843	1.186	1.548	0.223
104	0.145	10.87	1.256	0.796	1.253	0.228
121	0.132	12.54	1.455	0.687	1.138	0.219
139	0.111	17.56	1.896	0.528	1.025	0.215

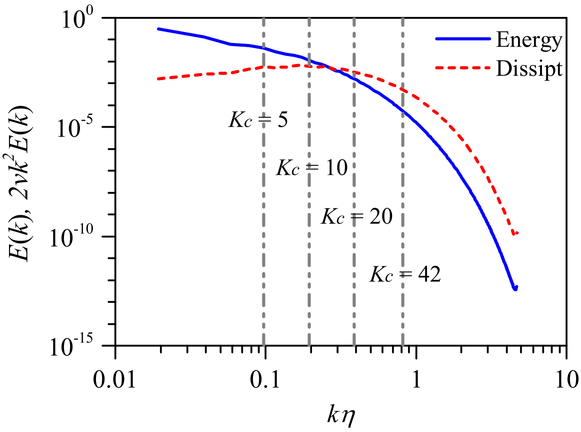

FIG. 7. Spectra for energy $E(k)$ (blue solid line) and energy dissipation $2\nu k^2 E(k)$ (red dashed line) with $R_\lambda = 104$. Vertical lines are drawn at different cutoff wave numbers K_c.

for the mitigation of preferential concentration of low-St particles as R_λ increases. It needs to be pointed out that the above analysis is based on the assumption that the particle number density is a continuous field. Therefore, Eq. (10) is only suitable for regions with high particle concentration, and it is not precise (only qualitative analysis) in regions with low particle concentration. Here Eq. (10) is only used as a semiquantitative analysis as we focus on the governing parameters that influence the level of particle clustering at different Reynolds number.

An aside, recall that τ_f is on the order of τ_η [27,28]. Then one might replace τ_f in Eq. (10) with τ_η,

$$n \approx n_0 e^{\tau_\eta^2 \langle Q \rangle_l \mathrm{St}}. \tag{11}$$

It is obvious that for a fixed St, there is a significant deviation between τ_f and τ_η, suggested by Table III. Additionally, replacing τ_f by τ_η, will lead to the conclusion that $\tau_f R_\lambda \sim \tau_\eta R_\lambda \sim T_f$, which is then essentially independent of R_λ. Simultaneously, $\langle Q \rangle_l/(R_\lambda)^2$ seems to be roughly unchanged with the increase of R_λ in our simulations, implied by Table III (cannot give a physical interpretation to this fact yet). Thus, the values of $\tau_\eta^2 \langle Q \rangle_l$ are quite close at different R_λ. With these caveats in mind, we believe that the approximation of Eq. (11) to Eq. (10) is inappropriate in understanding the Reynolds number dependence of particle clustering.

C. Reynolds number dependence at high St

Unlike the low-St case where the degree of particle clustering is suppressed when the Reynolds number increases, the high-St particle clustering is enhanced with increasing Reynolds number, see Fig. 1 in Sec. III A. This recalls the finding [56–59] that the particle clustering is scale-dependent. Namely, the preferential concentration of low-St and high-St particles is determined, respectively, by small- and large-scale eddies. It is natural then to inquire here as to whether varying Reynolds number could trigger different behavior of these coherent structures, e.g., different volume fractions of small- and large-scale eddies, thus providing clues to how the Reynolds number would affect the particle clustering.

The first point at hand is to justify the role of eddies on particle clustering again in our HIT system. To resolve fields in scales, we introduce a filtering operation that acts as a low-pass sharp Fourier filter at wave number K_c. Here four cut-off wave numbers, $K_c = 42$, 20, 10, and 5, are applied to the turbulence with $R_\lambda = 104$, which are drawn as vertical lines in Fig. 7. The corresponding scales $L_c = \pi/K_c$ of $K_c = 42$ and $K_c = 5$ are about 4η and up to the half of integral length scale, respectively. Particles uniformly distributed then evolve according to the filtered

TABLE IV. Summary of parameters for particle motions in filtered turbulence with $R_\lambda = 104$: cutoff wave number K_c, corresponding cutoff scale $L_c = 2\pi/K_c$, and Stokes number St.

Cases	K_c	$L_c = \pi/K_c$	St
C42_L	42	0.075	0.33
C42_H	42	0.075	6.40
C20_L	20	0.157	0.33
C20_H	20	0.157	6.40
C10_L	10	0.314	0.33
C10_H	10	0.314	6.40
C05_L	5	0.628	0.33
C05_H	5	0.628	6.40

velocity. Here we take two types of particles, i.e., St ≈0.33 and 6.40, as examples. For simplicity, an abbreviation is used to represent runs of different St particles under differently filtered turbulence. For example, "C42_L" represents particles with St ≈0.33 evolving in the filtered turbulence with $K_c = 42$. The relevant details are listed in Table IV.

Figure 8 shows the standard deviation σ_v at varying cutoff wave numbers K_c, for both low- (e.g., St ≈0.33) and high-St (e.g., St ≈6.40) particles. Obviously, they have the opposite bias: the preferential concentration of low-St particles is alleviated with the decrease of K_c [see also Figs. 9(a) and 9(b)]; while that of high-St particles is enhanced [see also Figs. 9(c) and 9(d)]. This indicates that eddies at different scales might contribute to low- and high-St particle clustering. The preferential concentration of high-St (low-St) particles is determined by large-scale (small-scale) eddies such that it is enhanced (mitigated) as more small-scale eddies are eliminated through filtering. Also noteworthy in Fig. 8 is that neither the standard deviation σ_v for high-St particles nor that for low-St particles at large cut-off wavenumbers (e.g., $K_c = 20$ and 42) exhibits apparent deviation from the unfiltered cases. Only when the filtering is applied at sufficiently small cutoff wave numbers, typically smaller than the wave number at which the dissipation spectrum reaches its maximum [58] (approximate to $k \approx 10$ in current case), the volume standard deviation shows significant dependence on K_c.

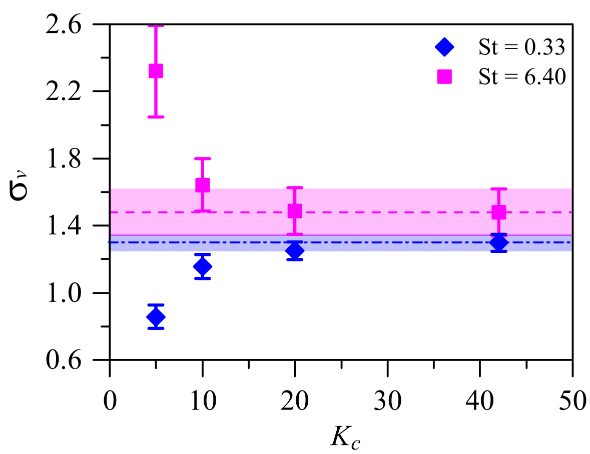

FIG. 8. The standard deviation σ_v for particles with St ≈0.33 and 6.40 at varying cutoff wave numbers K_c. σ_v for particles with St ≈0.33 and 6.40 in the unfiltered turbulence is plotted as a dashed line and a dash-dotted line, respectively, and the width of the shadow areas means the corresponding error range.

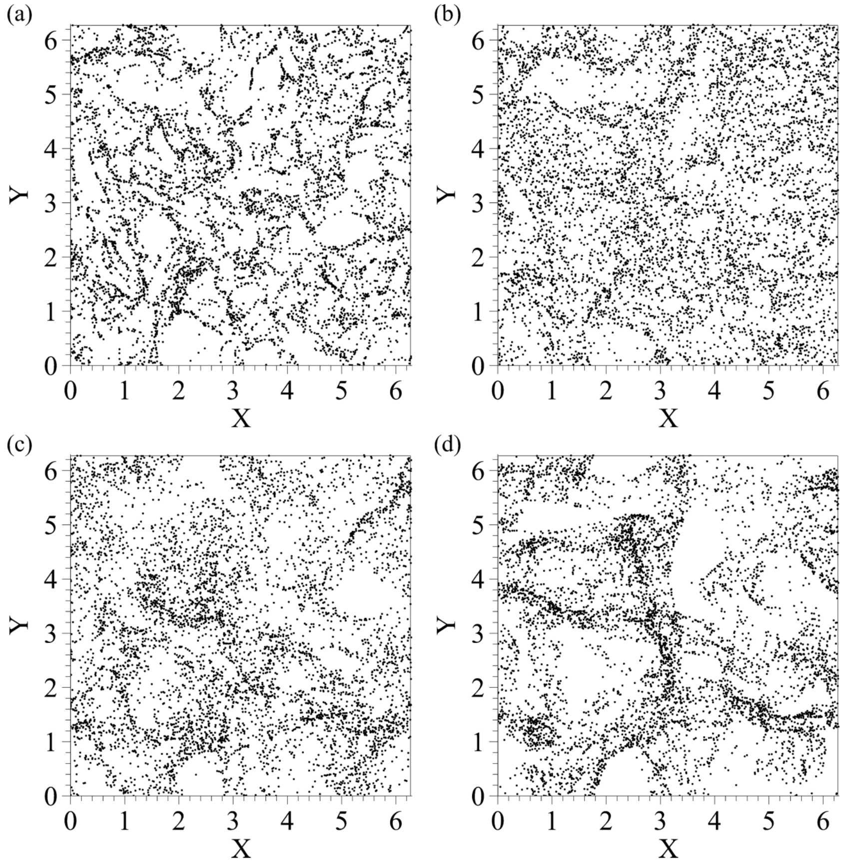

FIG. 9. Particle distribution in the same 2D slice for (a) C42_L, (b) C05_L, (c) C42_H, and (d) C05_H. For low St (a, b), the degree of particle clustering decreases with the reduction of K_c, while for high St (c, d), it increases as K_c decreases.

Upon clarifying the dominance of eddies on particle clustering, we move into the realm of its Reynolds number dependence. It is customary to expect that the turbulence with a higher Reynolds number contains larger (relative to the Kolmogorov length scale) and stronger eddies, which are responsible for the preferential concentration of high-St particles. We anticipate then that the high-St particle clustering becomes more intensive as the Reynolds number increases. This scenario also reconciles with the conjecture proposed by Goto and Vassilicos [56], in which they defined a scale-dependent Stokes number, $\mathrm{St}_r = \tau_p/\tau_r$, where $\tau_r = \varepsilon^{-1/3} \cdot r^{2/3}$ represents the turnover time of local eddy with size of r. The strongest local preferential concentration of particles tends to occur in localized patches with $\mathrm{St}_r \approx 1$, which corresponds to local eddies of certain size, let us say r_0. Increasing R_λ would presumably amplify the strength of large-scale eddies, thus leads to a higher probability for eddies with size comparable to r_0 and therefore stronger preferential concentration.

IV. CONCLUSION AND DISCUSSION

We have performed a quantitative assessment of the Reynolds number dependence of the preferential concentration of heavy inertial particles of size much smaller than the Kolmogorov length scale, in incompressible HIT using Voronoï method. In present paper, the influence of particles on turbulence and the interaction of particles are neglected. We find that for increasing Reynolds numbers, the preferential concentration of low-St particles is moderated, whereas it is the other way

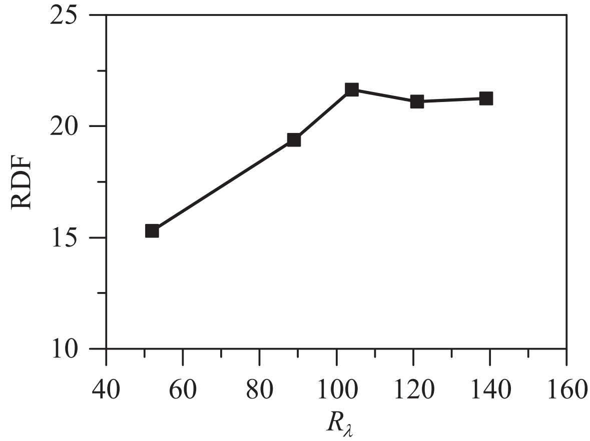

FIG. 10. RDF at contact for varying R_λ at St ≈1.25.

round for high-St particles, that is, its preferential concentration tends to be enhanced by elevated Reynolds numbers.

From Eq. (10) we can deduce that the low-St particle clustering could be associated with the Kolmogorov timescale (τ_η), the characteristic time (τ_f) of particles being trapped by "shear structures" and the strength of "shear structures" ($Q = S_{ij}S_{ij} - \Omega_{ij}\Omega_{ij}$). Then the outcome of incorporating the Reynolds number dependence of the three quantities will be closely related to the relative weighting of these dependencies. In our investigation, $\tau_\eta R_\lambda$ and $\langle Q\rangle_l/(R_\lambda)^2$ are roughly constant with the increase of R_λ. However $\tau_f R_\lambda$ decreases apparently with R_λ. Therefore, the degree of particle clustering decreases with the increasing R_λ. The above reasoning does not remain applicable to high-St particles. The preferential concentration of high-St particles is mainly controlled by large-scale eddies, and small-scale eddies whose lifetime are much shorter than the particle response time tend to randomize the particle distribution, acting to enhance turbulent diffusion. Consequently, the turbulence with higher Reynolds numbers, in possession of larger and stronger eddies, fosters the preferential concentration of high-St particles.

The studies [15,28,35,36] on the RDF of particles at contact have evidenced, instead, an enhancement of the preferential concentration of low-St particles for increasing Reynolds numbers as $R_\lambda < 100$. Balkovsky *et al.* [60] analyzed the fluctuation of particle concentration in viscous scale in detailed. An analytic statistical theory [18,60] could explain the performance of the RDF of particles at contact with R_λ. We plot the RDF of particles at contact as well using our DNS dataset, as shown in Fig. 10, which clearly reproduces similar trends as Rosa *et al.* [35], Onishi *et al.* [36], Onishi and Vassilicos [15]. So we inquire why we reach opposite conclusions by virtue of the Voronoï method and the RDF at contact. The reasons that we could come up with are essentially two: (i) the RDF at contact describes particle clustering at one scale, i.e., the particle diameter, which is always much smaller than the Kolmogorov length scale, while the Voronoï analysis assesses particle clustering without separately describing its behavior at different scales. (ii) To study the Reynolds number dependence of particle clustering, one should keep Stokes number constant by changing particle size. Usually different flow Reynolds numbers correspond to different particle sizes, which will inevitably change the RDF at contact. In this sense, the RDF at contact does not properly account for the Reynolds number effect since it is particle size dependent.

The most studied cases of particle clustering have been attributed to high strain and low rotation motions, at least in part due to the inspiration of Eq. (7) proposed by Maxey [11]. However, a more detailed treatment in this paper reveals that only the low rotation and not the high strain contributes directly to the preferential concentration of low-St particles. So how are our results to be reconciled with the previous studies that evidenced the association of particle clustering and high strain? For an empirical answer, we resort to the different degree of correlation between high strain and low rotation. In some studies [12,51–53], there is a very high degree of correlation between high strain and low rotation. Therefore, low-St particles populate around the peripheries of vortices where the low rotation and high strain are co-located. In our incompressible HIT, however, the region with low rotation is not in apparent association with the region with high strain.

There is a broad range of particle-laden turbulent systems, varying in characteristic parameters, may involving additional physical processes, for which valuable extensions of present study are sought. For example, our simulations clearly exhibit different behaviors of high- and low-St particles but nonetheless involve only a very limited Reynolds number range ($R_\lambda = 52 \sim 139$). We would expect our results to be justified in flows with higher Reynolds numbers. In addition, we fixed the particle number density in the computational domain over all simulations. Alternatively, if the particle number density based on Kolmogorov length scale is fixed, the results on Reynolds number dependence of particle clustering may be different via Voronoï analysis. we will devote to a future detailed study on this problem. It is also noteworthy that the reasoning for the Reynolds number dependence of particle clustering in this paper is not cast in a well-defined quantitative form. We therefore anticipate our results to be a starting point for more sophisticated models. Moreover, vorticity appears in bundles that are increasingly localized and isolated from each other as the Reynolds number increases. This intermittency might have an impact on the clustering of particles. But it is not taken into consideration in this paper. Finally, here we do not discuss the Reynolds number dependence of particle clustering at different scales (e.g., in dissipation range or in inertial range). One can imagine that this problem must be more complex than what we have described so far, which we will defer to a future study.

ACKNOWLEDGMENTS

This work is supported by the National Natural Science Foundation of China (Grants No. 91752201, No. 11672123, No. 91852205, No. 91741101, and No. 11961131006), the Department of Science and Technology of Guangdong Province (Grant No. 2019B21203001), and by the Shenzhen Science and Technology Innovation Committee (Grants No. JCYJ20170412151759222 and No. KQTD20180411143441009). We acknowledge computing support provided by the Center for Computational Science and Engineering of the Southern University of Science and Technology.

[1] M. R. Maxey and J. J. Riley, Equation of motion for a small rigid sphere in a nonuniform flow, Phys. Fluids **26**, 883 (1983).

[2] R. Gatignol, The faxén formulae for a rigid particle in an unsteady non-uniform Stokes flow, J. Méc. Théor. Appl. **1**, 143 (1983).

[3] A. B. Basset, *A Treatise on Hydrodynamics: With Numerous Examples*, Vol. 2 (Deighton, Bell and Company, London, 1888).

[4] J. Boussinesq, *Theorie Analytique de la Chaleur*, Vol. 2 (Gauthier-Villars, Paris, 1903).

[5] C. W. Oseen, *Neuere Methoden und Ergebnisse in der Hydrodynamik* (Akademische Verlagsgesellschaft mb H, Leipzig, 1927).

[6] C. Tchen, Equation of the motion for a particle suspended in an homogeneous field, Ph.D. thesis, Delft University, 1947.

[7] S. Corrsin and J. Lumley, On the equation of motion for a particle in turbulent fluid, Appl. Sci. Res., Sect. A **6**, 114 (1956).

[8] Y. A. Buevich, Motion resistance of a particle suspended in a turbulent medium, Fluid Dyn. **1**, 119 (1966).

[9] S. Soo, Equation of motion of a solid particle suspended in a fluid, Phys. Fluids **18**, 263 (1975).

[10] M. Gitterman and V. Steinberg, Memory effects in the motion of a suspended particle in a turbulent fluid, Phys. Fluids **23**, 2154 (1980).

[11] M. Maxey, The gravitational settling of aerosol particles in homogeneous turbulence and random flow fields, J. Fluid Mech. **174**, 441 (1987).
[12] K. D. Squires and J. K. Eaton, Preferential concentration of particles by turbulence, Phys. Fluids A **3**, 1169 (1991).
[13] S. Coleman and J. Vassilicos, A unified sweep-stick mechanism to explain particle clustering in two- and three-dimensional homogeneous, isotropic turbulence, Phys. Fluids **21**, 113301 (2009).
[14] Y. Tagawa, J. M. Mercado, V. N. Prakash, E. Calzavarini, C. Sun, and D. Lohse, Three-dimensional Lagrangian Voronoï analysis for clustering of particles and bubbles in turbulence, J. Fluid Mech. **693**, 201 (2012).
[15] R. Onishi and J. Vassilicos, Collision statistics of inertial particles in two-dimensional homogeneous isotropic turbulence with an inverse cascade, J. Fluid Mech. **745**, 279 (2014).
[16] A. D. Bragg, P. J. Ireland, and L. R. Collins, Mechanisms for the clustering of inertial particles in the inertial range of isotropic turbulence, Phys. Rev. E **92**, 023029 (2015).
[17] A. D. Bragg, P. J. Ireland, and L. R. Collins, On the relationship between the non-local clustering mechanism and preferential concentration, J. Fluid Mech. **780**, 327 (2015).
[18] G. Falkovich, A. Fouxon, and M. G. Stepanov, Acceleration of rain initiation by cloud turbulence, Nature **419**, 151 (2002).
[19] J. Bec, A. Celani, M. Cencini, and S. Musacchio, Clustering and collisions of heavy particles in random smooth flows, Phys. Fluids **17**, 073301 (2005).
[20] M. Wilkinson and B. Mehlig, Caustics in turbulent aerosols, Europhys. Lett. **71**, 186 (2005).
[21] M. Wilkinson, B. Mehlig, and V. Bezuglyy, Caustic Activation of Rain Showers, Phys. Rev. Lett. **97**, 048501 (2006).
[22] J. Chun, D. L. Koch, S. L. Rani, A. Ahluwalia, and L. R. Collins, Clustering of aerosol particles in isotropic turbulence, J. Fluid Mech. **536**, 219 (2005).
[23] L. I. Zaichik and V. M. Alipchenkov, Refinement of the probability density function model for preferential concentration of aerosol particles in isotropic turbulence, Phys. Fluids **19**, 113308 (2007).
[24] A. D. Bragg and L. R. Collins, New insights from comparing statistical theories for inertial particles in turbulence: I. Spatial distribution of particles, New J. Phys. **16**, 055013 (2014).
[25] S. Goto and J. C. Vassilicos, Sweep-Stick Mechanism of Heavy Particle Clustering in Fluid Turbulence, Phys. Rev. Lett. **100**, 054503 (2008).
[26] L.-P. Wang and M. R. Maxey, Settling velocity and concentration distribution of heavy particles in homogeneous isotropic turbulence, J. Fluid Mech. **256**, 27 (1993).
[27] Y. Zhou, A. S. Wexler, and L.-P. Wang, On the collision rate of small particles in isotropic turbulence. II. Finite inertia case, Phys. Fluids **10**, 1206 (1998).
[28] L.-P. Wang, A. S. Wexler, and Y. Zhou, Statistical mechanical description and modeling of turbulent collision of inertial particles, J. Fluid Mech. **415**, 117 (2000).
[29] H. Yoshimoto and S. Goto, Self-similar clustering of inertial particles in homogeneous turbulence, J. Fluid Mech. **577**, 275 (2007).
[30] J. Bec, L. Biferale, M. Cencini, A. Lanotte, S. Musacchio, and F. Toschi, Heavy Particle Concentration in Turbulence at Dissipative and Inertial Scales, Phys. Rev. Lett. **98**, 084502 (2007).
[31] J. Bec, M. Cencini, R. Hillerbrand, and K. Turitsyn, Stochastic suspensions of heavy particles, Physica D **237**, 2037 (2008).
[32] T. Hartlep, J. N. Cuzzi, and B. Weston, Scale dependence of multiplier distributions for particle concentration, enstrophy, and dissipation in the inertial range of homogeneous turbulence, Phys. Rev. E **95**, 033115 (2017).
[33] R. C. Hogan and J. N. Cuzzi, Stokes and Reynolds number dependence of preferential particle concentration in simulated three-dimensional turbulence, Phys. Fluids **13**, 2938 (2001).
[34] L. R. Collins and A. Keswani, Reynolds number scaling of particle clustering in turbulent aerosols, New J. Phys. **6**, 119 (2004).
[35] B. Rosa, H. Parishani, O. Ayala, W. W. Grabowski, and L.-P. Wang, Kinematic and dynamic collision statistics of cloud droplets from high-resolution simulations, New J. Phys. **15**, 045032 (2013).

[36] R. Onishi, K. Takahashi, and J. C. Vassilicos, An efficient parallel simulation of interacting inertial particles in homogeneous isotropic turbulence, J. Comput. Phys. **242**, 809 (2013).

[37] S. Sumbekova, A. Cartellier, A. Aliseda, and M. Bourgoin, Preferential concentration of inertial sub-kolmogorov particles: The roles of mass loading of particles, Stokes numbers, and Reynolds numbers, Phys. Rev. Fluids **2**, 024302 (2017).

[38] S. A. Orszag, Comparison of pseudospectral and spectral approximation, Stud. Appl. Math. **51**, 253 (1972).

[39] C. Canuto, M. Y. Hussaini, A. Quarteroni, A. Thomas Jr. *et al.*, *Spectral Methods in Fluid Dynamics* (Springer Science & Business Media, Berlin, 2012).

[40] E. Hairer, S. P. Nørsett, and G. Wanner, *Solving Ordinary Differential Equations. 1. Nonstiff Problems* (Springer-Verlag, Berlin, 1991).

[41] J. C. Butcher, *Numerical Methods for Ordinary Differential Equations* (John Wiley & Sons, New York, 2016).

[42] S. Balachandar and J. K. Eaton, Turbulent dispersed multiphase flow, Annu. Rev. Fluid Mech. **42**, 111 (2010).

[43] J.-S. Ferenc and Z. Néda, On the size distribution of Poisson Voronoi cells, Physica A **385**, 518 (2007).

[44] R. Monchaux, M. Bourgoin, and A. Cartellier, Preferential concentration of heavy particles: A Voronoï analysis, Phys. Fluids **22**, 103304 (2010).

[45] R. Monchaux, M. Bourgoin, and A. Cartellier, Analyzing preferential concentration and clustering of inertial particles in turbulence, Int. J. Multiphase Flow **40**, 1 (2012).

[46] L. Fiabane, R. Zimmermann, R. Volk, J.-F. Pinton, and M. Bourgoin, Clustering of finite-size particles in turbulence, Phys. Rev. E **86**, 035301(R) (2012).

[47] A. Ferrante and S. Elghobashi, On the physical mechanisms of two-way coupling in particle-laden isotropic turbulence, Phys. Fluids **15**, 315 (2003).

[48] G. Jin, Y. Wang, J. Zhang, and G. He, Turbulent clustering of point particles and finite-size particles in isotropic turbulent flows, Ind. Eng. Chem. Res. **52**, 11294 (2013).

[49] S. Elghobashi, Direct numerical simulation of turbulent flows laden with droplets or bubbles, Annu. Rev. Fluid Mech. **51**, 217 (2019).

[50] R. Monchaux, Measuring concentration with Voronoï diagrams: The study of possible biases, New J. Phys. **14**, 095013 (2012).

[51] J. K. Eaton and J. Fessler, Preferential concentration of particles by turbulence, Int. J. Multiphase Flow **20**, 169 (1994).

[52] L. R. Sundaram and S. Collins, Collision statistics in an isotropic particle-laden turbulent suspension. Part 1. Direct numerical simulations, J. Fluid Mech. **335**, 75 (1997).

[53] M. H. Kasbaoui, D. L. Koch, and O. Desjardins, Clustering in Euler–Euler and Euler–Lagrange simulations of unbounded homogeneous particle-laden shear, J. Fluid Mech. **859**, 174 (2019).

[54] J. Jiménez, A. A. Wray, P. G. Saffman, and R. S. Rogallo, The structure of intense vorticity in isotropic turbulence, J. Fluid Mech. **255**, 65 (1993).

[55] R. Onishi and A. Seifert, Reynolds-number dependence of turbulence enhancement on collision growth, Atmos. Chem. Phys. Discuss. **16**, 12441 (2016).

[56] S. Goto and J. Vassilicos, Self-similar clustering of inertial particles and zero-acceleration points in fully developed two-dimensional turbulence, Phys. Fluids **18**, 115103 (2006).

[57] J. Bec, L. Biferale, M. Cencini, A. Lanotte, and F. Toschi, Intermittency in the velocity distribution of heavy particles in turbulence, J. Fluid Mech. **646**, 527 (2010).

[58] B. Ray and L. R. Collins, Preferential concentration and relative velocity statistics of inertial particles in Navier–Stokes turbulence with and without filtering, J. Fluid Mech. **680**, 488 (2011).

[59] Y. Xiong, J. Li, Z. Liu, and C. Zheng, The influence of sub-grid scale motions on particle collision in homogeneous isotropic turbulence, Acta Mech. Sin. **34**, 22 (2018).

[60] E. Balkovsky, G. Falkovich, and A. Fouxon, Intermittent Distribution of Inertial Particles in Turbulent Flows, Phys. Rev. Lett. **86**, 2790 (2001).